

PHYSICAL PARAMETERS OF THE AFTERGLOWS OF GRB 980703, 990123, 990510, AND 991216
DETERMINED FROM MODELING OF MULTI-FREQUENCY DATA

A. PANAITESCU

Dept. of Astrophysical Sciences, Princeton University, Princeton, NJ 08544

AND

P. KUMAR

Institute for Advanced Study, Olden Lane, Princeton, NJ 08540

ABSTRACT

We model the radio, optical, and X -ray emission for the afterglows of GRB 980703, 990123, 990510, and 991216, within the framework of relativistic jets, to determine the physical parameters of these afterglows. For the last three we find jet energies around 10^{51} ergs and initial opening angles less than 3 deg. The external medium density obtained from fits to the data ranges from 10^{-4} cm^{-3} to less than 1 cm^{-3} . Our results show that, for these four afterglows, the uncertainty in the remnant isotropic equivalent energy and in the external medium density is about one order of magnitude. If the energy per solid angle in the ejecta is uniform (i.e. has no angular dependence), then the radiative efficiency during the GRB phase must have been at least 0.3% for GRB 980703, 2% for GRB 990510, 4% for GRB 991216, and 8% for GRB 990123.

Subject headings: gamma-rays: bursts - ISM: jets and outflows - methods: numerical - radiation mechanisms: non-thermal - shock waves

1. INTRODUCTION

There are two basic quantities one needs to try understanding the nature of any astronomical source – the distance and the energy of the source. For the long duration GRBs, lasting for $\gtrsim 10$ seconds, the former is well established to be cosmological. However, the energy associated with the GRBs remains uncertain.

The efficiency for producing γ -ray emission for the generally accepted internal shock model (Mészáros & Rees 1994), which can explain the observed temporal variability, is less than a few percent (Kumar 1999, Lazzati, Ghisellini & Celotti 1999, Panaitescu, Spada & Mészáros 1999, see also Beloborodov 2000). This suggests that the total energy in the explosion is larger than the energy observed in γ -rays by a factor of at least 20–50.

The goal of this work is to infer the physical parameters of the ejecta, including their energy and the external medium density, from modeling of radio, optical and X -ray data for GRB afterglows with known redshifts. The modeling is carried out in the framework of collimated ejecta interacting with an isotropic external medium. The model is described in §2 and the results of the numerical calculations for individual afterglows are given in §4.

2. DESCRIPTION OF THE MODEL

In calculating the jet dynamics, we assume that the energy and baryon density within the ejecta do not have an angular dependence, and that the external medium is isotropic. We also assume that, at any time, the swept up external gas has the same physical parameters, and moves at the same Lorentz factor Γ . We include the effect of radiative energy loss on the jet dynamics.

For the calculation of synchrotron emission, we assume a tangled magnetic field and that the electrons accelerated at shock have a power-law distribution. We assume that the electron distribution resulting from the continuous injection at shock and adiabatic+radiative cooling is a broken power-law,

with a break at the minimum random Lorentz factor of the freshly injected electrons and another one at the cooling electron Lorentz factor. Furthermore, in calculating the received flux, the swept up gas is approximated as a surface, i.e. the thickness of the emitting shell is ignored. The effect of the remnant curvature on the photon arrival time and energy is taken into account.

2.1. Dynamics

The interaction between the relativistic ejecta that generated the GRB with the external gas continuously decelerates the jet and heats the newly swept up gas. Assuming that the heated gas has a uniform temperature, equal to that of the freshly shocked fluid, the total energy of the remnant can be written as:

$$E(r) = m(r)(\Gamma^2 - 1) + m_0(\Gamma - 1), \quad (1)$$

where m_0 is the mass of the ejecta, Γ_0 is their initial Lorentz factor (i.e. at the end of the GRB phase), corresponding to initial energy $E_0 = (\Gamma_0 - 1)m_0c^2$, and E is the current total energy of the jet.

In the above equation, m is the mass of the swept up external gas, given by

$$dm(r) = \Omega(r)\rho(r)r^2 dr, \quad (2)$$

where $\rho(r) \propto r^{-s}$ is the external medium density ($s = 0$ for homogeneous gas, $s = 2$ for a wind ejected at constant speed before the release of the ultra-relativistic ejecta), and $\Omega(r)$ is solid angle of the jet.

The jet half opening angle increases due to the lateral spreading of the jet at the local sound speed c_s :

$$r d\theta = c_s dt' = \Gamma^{-1} c_s dt_{lab}, \quad (3)$$

t' and t_{lab} being the time measured in the ejecta comoving and laboratory frames, respectively. The speed of sound is

$$c_s^2 = \frac{\hat{\gamma}(\hat{\gamma} - 1)u'}{\rho' + \hat{\gamma}u'} = \frac{\hat{\gamma}(\hat{\gamma} - 1)(\Gamma - 1)}{1 + \hat{\gamma}(\Gamma - 1)}, \quad (4)$$

where $u' = (\Gamma - 1)\rho'$ and ρ' are the comoving internal energy and rest mass densities, respectively, and $\hat{\gamma}$ is the adiabatic index. In the relativistic limit $\hat{\gamma} = 4/3$ and $c_s = 1/\sqrt{3}$, while for non-relativistic speeds $\hat{\gamma} = 5/3$ and $c_s = (\sqrt{5}/3)v$, where v is the radial expansion speed. We relate the adiabatic index with Γ through a simple formula, which has the above asymptotic limits. Numerical calculations of afterglow light-curves show that the sideways expansion speed has little effect on the received emission as long as $v \gtrsim 0.2c$.

The energy loss through synchrotron and inverse Compton emissions is given by

$$\frac{dE}{dt_{lab}} = -\frac{1}{6\pi}\sigma_T c B^2 (Y + 1) \int_{\gamma_m}^{\gamma_M} \gamma^2 d\mathcal{N}(\gamma), \quad (5)$$

where B is the magnetic field intensity, Y the Compton parameter, \mathcal{N} is the normalized electron distribution (§2.2), and γ is the electron random Lorentz factor.

Equations (1), (2), (3) and (5) are solved numerically, subject to the boundary conditions: $\Gamma(0) = \Gamma_0$, $m(0) = 0$, $\theta(0) = \theta_0$, and $E(0) = E_0$.

2.2. Electron Distribution and Spectral Breaks

The magnetic field intensity is parameterized relative to its equipartition value

$$B^2 = 8\pi\rho'c^2(\Gamma - 1)\varepsilon_B = 32\pi\rho(r)c^2(\Gamma - 1)\frac{\hat{\gamma}\Gamma + 1}{\hat{\gamma} - 1}, \quad (6)$$

where ρ' is the comoving frame rest-mass density.

The distribution of the electrons accelerated by the forward shock and injected in down-stream is assumed to be a power-law of index p

$$\mathcal{N}_i(\gamma) \propto \gamma^{-p}, \quad \gamma_i < \gamma < \gamma_M, \quad (7)$$

where γ_i is the minimum, injected electron Lorentz factor, parameterized relative to its value at equipartition,

$$\gamma_i = \epsilon_e \frac{m_p}{m_e}(\Gamma - 1), \quad (8)$$

and γ_M is an upper limit, determined by the conditions that the acceleration timescale of such electrons does not exceed the radiative loss timescale, and that the total energy in the injected electrons does not exceed a certain fraction ε_{max} of the available internal energy. The former leads to

$$\gamma_M^{(1)} = \left[\frac{3e}{n_g \sigma_T B (Y + 1)} \right]^{1/2}, \quad (9)$$

where n_g is the ratio of the acceleration timescale to the gyration time. The latter condition can be written as

$$m_e \int_{\gamma_i}^{\gamma_M^{(2)}} \gamma d\mathcal{N}_i(\gamma) = \varepsilon_{max} m_p(\Gamma - 1), \quad (10)$$

where \mathcal{N}_i is normalized (to unity), and m_e and m_p are the electron and proton mass, respectively. Equation (10) leads to a transcendental equation which can be solved numerically. The γ_M is the minimum between $\gamma_M^{(1)}$ and $\gamma_M^{(2)}$ above. For numerics we shall use $n_g = 10$ and $\varepsilon_{max} = 0.5$.

The upper limit given by equation (9) is sufficiently large that the synchrotron emission from $\gamma_M^{(1)}$ -electrons is at frequencies above the X -ray domain. For $p < 3$ this upper limit could be important in determining the Compton parameter (see below). For $p < 2$ and $2 \lesssim p < 3$, or if $\varepsilon_e \lesssim \varepsilon_{max}$, the upper limit given by equation (10) may be sufficiently low as to yield a cut-off of the afterglow emission at the higher frequencies of interest (X -rays and even optical).

The distribution of cooled electrons is a power-law of index 2 if the electrons are cooling faster than the dynamical timescale, and a power-law steeper by unity than the injected distribution in the opposite case. Therefore the electron distribution resulting from injection at shock and radiative cooling is (Sari, Piran & Narayan 1998):

$$\mathcal{N}(\gamma) \propto \begin{cases} \gamma^{-2} & \gamma_c < \gamma < \gamma_i \\ \gamma^{-(p+1)} & \gamma_i < \gamma \end{cases}, \quad (11)$$

for fast cooling electrons ($\gamma_c < \gamma_i$), and

$$\mathcal{N}(\gamma) \propto \begin{cases} \gamma^{-p} & \gamma_i < \gamma < \gamma_c \\ \gamma^{-(p+1)} & \gamma_c < \gamma \end{cases}, \quad (12)$$

for slow cooling electrons ($\gamma_i < \gamma_c$). In equations (11) and (12), γ_c is the cooling electron Lorentz factor, defined by the equality of its radiative cooling timescale with the dynamical timescale:

$$\gamma_c = \frac{6\pi m_e c}{\sigma_T t' B^2 (Y + 1)}. \quad (13)$$

The Compton parameter Y is given by (Panaitescu & Kumar 2000)

$$Y = \frac{4}{3} \tau_e \int_{\gamma_m}^{\gamma_M} \gamma^2 d\mathcal{N}(\gamma), \quad (14)$$

where $\gamma_m = \min(\gamma_i, \gamma_c)$ and τ_e is the optical thickness to electron scattering:

$$\tau_e = \frac{1}{4\pi} \frac{\sigma_e m(r)}{m_p r^2}. \quad (15)$$

We take into account the Klein-Nishina reduction by setting an upper limit γ_{KN} to the integral in equation (14) if $\gamma_{KN} < \gamma_M$, with γ_{KN} calculated as the geometric mean of the electron Lorentz factor $\gamma_{KN}^{(1)}$ for which up-scattering of its own synchrotron photons occurs at the Klein-Nishina limit, i.e. $\gamma_{KN}^{(1)} h\nu'(\gamma_{KN}^{(1)}) = m_e c^2$, and of the electron Lorentz factor $\gamma_{KN}^{(2)}$ corresponding to up-scattering of the synchrotron photons of γ_m -electrons at the same limit, i.e. $\gamma_{KN}^{(2)} h\nu'(\gamma_m) = m_e c^2$, with

$$\nu'(\gamma) = \frac{3e^2 B}{16 m_e c} \gamma^2. \quad (16)$$

The synchrotron self-absorption frequency in the fluid rest frame is at $\nu'_a = \nu'(\gamma_a)$ with $\nu'(\gamma)$ as given in equation (16), and γ_a given by (see Panaitescu & Kumar 2000)

$$\gamma_a = \left(\frac{5e\tau_e}{\sigma_T B} \right)^{3/10} \gamma_m^{-1/2}. \quad (17)$$

This equation is valid only if $\gamma_a < \gamma_m$.

2.3. Received Flux

The synchrotron spectrum is approximated as piece-wise power-law (see Sari et al. 1998) with breaks at the injection, cooling, and absorption breaks given by equations (16), (8), (13), and (17).

To calculate the afterglow flux seen by the observer, we consider that the emitting shell is infinitely thin and that the observer is located on the jet axis. Consider an annular region of area $\delta A = 2\pi r^2 \delta\mu$, with $\mu = \cos\omega$, where ω is the polar angle, measured relative to the jet axis. The energy emitted in the co-moving frame per unit time and frequency is $\delta L'_{\nu'} = P'_{\nu'} \Sigma_e \delta A$, where $P'_{\nu'}$ is the radiative comoving power per electron and Σ_e is the electron surface density. The infinitesimal comoving energy emitted per solid angle $(1/4\pi)\delta L'_{\nu'} d\nu' dt'$ is relativistically beamed toward the observer by a factor \mathcal{D}^2 and boosted in frequency by a factor \mathcal{D} , where $\mathcal{D} = [\Gamma(1 - \beta\mu)]^{-1}$, with $\beta = v/c$. Therefore the infinitesimal flux dF_{ν} received by the observer at frequency $\nu = \mathcal{D}\nu'$, during $\Delta t = c^{-1}r\delta\mu$ satisfies

$$dF_{\nu} d\nu \delta t = \frac{1+z}{4\pi d_L^2} \mathcal{D}^3 P'_{\nu'} \Sigma_e dt' d\nu' \delta A. \quad (18)$$

The flux received by the observer at time t is that given by equation (18) integrated over the entire evolution of the remnant. Using $dt' = dt_{lab}/\Gamma = dr/(\beta c\Gamma)$ and relating the electron surface density to the jet mass and area, $\Sigma_e = [m(r)/m_p]/(\Omega r^2)$, equation (18) leads to

$$F_{\nu}(t) = \frac{1+z}{2m_p d_L^2} \int \frac{dr}{\beta\Gamma^3(1-\beta\mu)^2} \frac{P'_{\nu'}(r)m(r)}{r\Omega(r)}, \quad (19)$$

with μ given by the condition that light emitted from location (r, μ) arrives at observer at time $t = t_{lab} - c^{-1}r\mu$. Thus equation (19) takes into account the spread in the photon arrival time due to the spherical curvature of the jet surface.

In equation (19) z is the afterglow redshift and d_L is the luminosity distance. In our calculations we shall assume a Universe with $H_0 = 65 \text{ km s}^{-1} \text{Mpc}^{-1}$, $q_0 = 0.1$, and $\Lambda = 0$.

3. ANALYTICAL CONSIDERATIONS

So far there are five afterglows for which a break in the optical emission has been identified. In all these cases the break is seen at or after $t = 1$ day. Within the framework of uniform ejecta interacting with isotropic media, there are two possible causes for such a break: the passage of a break frequency (injection – ν_i , or cooling – ν_c), or effects due to collimation of ejecta.

One can show that, within a factor of order unity, the break frequency ν_i is the same for both types of external medium:

$$\nu_i \sim 10^{13} (z+1)^{1/2} E_{0,54}^{1/2} \varepsilon_{e,-1}^{1/2} \varepsilon_{B,-2}^{1/2} t_d^{-3/2} \text{ Hz}, \quad (20)$$

where t_d is observer time in days, and the usual notation $A_n = 10^{-n} A$ was used. Equation (20) shows that, unless the isotropic equivalent energy exceeds 10^{56} ergs and the magnetic field is close to equipartition (ε_e cannot be much higher than 0.1, as the total fractional energy in electrons $[(p-1)/(p-2)]\varepsilon_e$ would be too large), ν_i is below the optical range at $t \gtrsim 1$ day. Therefore it is very unlikely that the light-curve breaks are due to the passage of ν_i through the observational band. Moreover, if this were the case, then, at times before the light-curve break, the temporal index α of the light-curve decay $-F_{\nu}(t) \propto t^{-\alpha}$ would be at most 1/4, which is much smaller than the observed α 's.

3.1. Passage of the Cooling Break

We consider here the afterglow emission at early times, when the effects due to collimation of ejecta are negligible, but sufficiently large that $\nu_i < \nu$. In this case, the afterglow light-curves for slow cooling electrons ($\nu_i < \nu_c$) are given by (see Panaitescu & Kumar 2000)

$$F_{\nu > \nu_i} \propto \begin{cases} t^{-(3p-3)/4} & \nu < \nu_c \\ t^{-(3p-2)/4} & \nu_c < \nu, Y < 1 \\ t^{-(3p/4)+1/(4-p)} & \nu_c < \nu, Y > 1, 2 < p < 3 \\ t^{-(3p/4)+1} & \nu_c < \nu, Y > 1, 3 < p \end{cases} \quad (21)$$

for a homogeneous external medium ($s = 0$), where the last two rows represent the case when the electron cooling is dominated by inverse Compton scatterings. For a pre-ejected wind ($s = 2$) and slow cooling electrons

$$F_{\nu > \nu_i} \propto \begin{cases} t^{-(3p-1)/4} & \nu < \nu_c \\ t^{-(3p-2)/4} & \nu_c < \nu, Y < 1 \\ t^{-(3p/4)+p/(8-2p)} & \nu_c < \nu, Y > 1, 2 < p < 3 \\ t^{-(3p/4)+3/2} & \nu_c < \nu, Y > 1, 3 < p \end{cases} \quad (22)$$

The second row of equations (21) and (22) also gives the light-curve for $\nu_i < \nu$ and fast cooling electrons.

The temporal evolution of the cooling break frequency ν_c for $s = 0$ and slow cooling electrons is given by

$$\nu_c \propto \begin{cases} t^{-1/2} & Y < 1 \\ t^{-(8-3p)/(8-2p)} & Y > 1, 2 < p < 3 \\ t^{1/2} & Y > 1, 3 < p \end{cases} \quad (23)$$

For $s = 2$ and slow cooling electrons

$$\nu_c \propto \begin{cases} t^{1/2} & Y < 1 \\ t^{(3p-4)/(8-2p)} & Y > 1, 2 < p < 3 \\ t^{5/2} & Y > 1, 3 < p \end{cases} \quad (24)$$

The first row also gives the evolution of ν_c for fast cooling electrons, in which case Y is time-independent.

Equation (23) shows that for $s = 0$ ν_c increases in time if the electron cooling is dominated by inverse Compton and if $p > 8/3$. From equation (21), the passage of ν_c through the observational band changes the light-curve decay index by

$$(\Delta\alpha)_c = \begin{cases} 1/4 & Y < 1 \\ (8-3p)/(16-4p) & Y > 1, 2 < p < 8/3 \\ (3p-8)/(16-4p) & Y > 1, 8/3 < p < 3 \\ 1/4 & Y > 1, 3 < p \end{cases} \quad (25)$$

Note $(\Delta\alpha)_c > 0$, i.e. the passage of ν_c always steepens the light-curve decay, even if ν_c increases in time, and that $(\Delta\alpha)_c < 1/4$. In the case where ν_c is above optical and below X-ray, the temporal indices of the X-ray and optical light-curves differ by $\alpha_x - \alpha_o = (\Delta\alpha)_c > 0$ if ν_c decreases in time, and by $\alpha_x - \alpha_o = -(\Delta\alpha)_c < 0$ if ν_c increases in time. Therefore, for $s = 0$, the X-ray emission decays faster than the optical one only if $Y < 1$ or if $Y > 1$ and $p < 8/3$.

For $s = 2$ equation (24) shows that ν_c always increases in time. From equation (22), the passage of ν_c yields

$$(\Delta\alpha)_c = \begin{cases} 1/4 & Y < 1 \\ (3p-4)/(16-4p) & Y > 1, 2 < p < 3 \\ 5/4 & Y > 1, 3 < p \end{cases} \quad (26)$$

Note that $1/4 < (\Delta\alpha)_c < 5/4$. For $\nu_o < \nu_c < \nu_x$, the X -ray and optical indices differ by $\alpha_x - \alpha_o = -(\Delta\alpha)_c < 0$. Therefore, if $s = 2$, the X -ray emission always decays slower than the optical one.

3.2. Collimation of Ejecta

If the ejecta is collimated (Rhoads 1999), the decay of the afterglow emission steepens after the time t_j when $\Gamma\theta = 1$. For $s = 0$

$$t_j = 0.26 (z + 1) (E_{0,54} \Omega_{0,-2}^4 n_0^{-1})^{1/3} \text{ day} . \quad (27)$$

The coefficient above was determined numerically, and is larger by a factor ~ 3 than that which is obtained analytically by assuming a constant θ at $t < t_j$. For $t > t_j$ the light-curve decay is asymptotically approaching $F_\nu \propto t^{-p}$ at frequencies above ν_i , irrespective of the location of ν_c . This result ignores a multiplying term which is logarithmic in the jet radius and, with the same approximation, also holds for a jet interacting with a pre-ejected wind. Furthermore, this result is valid only at times when the remnant is sufficiently relativistic. From numerical results we find that the decay index α is approximated by p with an error less than 10% if $\Gamma \gtrsim 10$. It is quite possible that, at times after the optical light-curve break was seen in the emission of some afterglows, this condition is not satisfied.

Using equations (21) and (22), it can be shown that, at $\nu > \nu_i$, the magnitude of the break due to collimation of ejecta is

$$(\Delta\alpha)_j = \begin{cases} (p+3)/4 & \nu < \nu_c \\ (p+2)/4 & \nu_c < \nu, Y < 1 \\ p/4 + 1/(4-p) & \nu_c < \nu, Y > 1, 2 < p < 3 \\ (p+4)/4 & \nu_c < \nu, Y > 1, 3 < p \end{cases} . \quad (28)$$

for $s = 0$ and

$$(\Delta\alpha)_j = \begin{cases} (p+1)/4 & \nu < \nu_c \\ (p+2)/4 & \nu_c < \nu, Y < 1 \\ p/4 + p/(8-2p) & \nu_c < \nu, Y > 1, 2 < p < 3 \\ (p+4)/4 & \nu_c < \nu, Y > 1, 3 < p \end{cases} . \quad (29)$$

for $s = 2$. The finite opening of the ejecta yields $\Delta\alpha = 3/4$ for $s = 0$ and $\Delta\alpha = 1/2$ for $s = 2$ (Panaitescu, Mészáros & Rees 1998) when the jet edge becomes visible, the remainder of the steepening being due to the sideways expansion of the jet (Kumar & Panaitescu 2000). Equations (28) and (29) show that, for $p > 2$, $(\Delta\alpha)_j > 1$ for $s = 0$ and $(\Delta\alpha)_j > 3/4$.

3.3. What Can We Infer from the X -ray and Optical Decay Indices?

The most important difference between a break due to passage of ν_c and one due to collimation of ejecta is the high chromaticity of the former, and the achromaticity of the latter. This would be the best criterion to distinguish between them if optical and X -ray observations spanning the same 1–2 decades in time, around the time when the break is seen, are available.

The analytical results presented in §3.1 and §3.2 allow us to draw some conclusions even when the existence of simultaneous X -ray and optical light-curve breaks cannot be clearly established. Equations (25), (26), (28), and (29) show that optical break magnitudes $\Delta\alpha < 3/4$ can be produced only by the passage of the cooling break, while $\Delta\alpha > 5/4$ can be due only to collimation of ejecta. The caveat of these criteria is that, as

shown by Kumar & Panaitescu (2000), for collimated ejecta, the completion of most of $(\Delta\alpha)_j$ is spread over at least 1.5 decades in observer time for $s = 0$ and over at least 2.5 decades for $s = 2$. Therefore observations spanning a shorter time range may underestimate the true magnitude of the jet edge break.

The results presented in §3.1 and §3.2 lead to the following criteria for determining the location of ν_c relative to the optical and X -ray domains, and for identifying the type of external medium:

1. if $\alpha_o = \alpha_x$, then either ν_c is not between the optical and X -ray domains, or it is in this range but is quasi-constant in time. The latter may occur either in collimated ejecta during the sideways expansion phase (Sari, Piran & Halpern 1999), or before jet edge effects are important, in $s = 0$ models, if the inverse Compton cooling is the dominant process and if $p \simeq 8/3$ (see eq. [23]).
2. if $\alpha_x > \alpha_o$ (i.e. the X -ray decay faster than the optical decay), then $\nu_o < \nu_c < \nu_x$ and the external medium must be homogeneous.
3. if $\alpha_x < \alpha_o$, then $\nu_o < \nu_c < \nu_x$ and either the external medium is a pre-ejected wind or it is homogeneous and the electron cooling is inverse Compton-dominated ($Y > 1$), with $p > 8/3$.

Using the observed spectral slope in the optical range and the relative intensity of the X -ray and optical emission, one can eliminate some of the above cases, and further reduce the number of potentially good models.

4. INDIVIDUAL AFTERGLOWS

The modeling of GRB afterglow light-curves is carried out by solving numerically equations (1), (2), (3), and (5), to determine the dynamics of the remnant and equation (19) to calculate the observed flux. The six unknown parameters E_0 , θ_0 , n , p , ϵ_e and ϵ_B , are varied to minimize the χ^2 between the observed and the theoretically calculated fluxes at the frequencies where most of the data for each afterglow is available.

In this work we restrict our attention to four afterglows for which radio, optical, X -ray light-curves and redshifts are available: GRB 980703, GRB 990123, GRB 990510, and GRB 991216, leaving out GRB 970508, whose optical light-curve cannot be entirely explained within the framework of our model, as it exhibited a brightening after 1 day, indicating a possible delayed energy injection, or fluctuations of the energy release parameters ϵ_e , ϵ_B or of the external density n .

For the selected afterglows, the optical magnitudes are converted to fluxes using the characteristics of photometric bands published by Fukugita, Shimasaku & Ichikawa (1995). For near-infrared (NIR) magnitudes, we used the conversion factors of Campins, Rieke, & Lebofsky (1985), and assumed a 5% uncertainty in the magnitude–flux conversion. The NIR and optical fluxes are corrected for dust extinction using the interstellar reddening curves of Mathis (1990), Schild (1977), and Cardelli, Clayton, & Mathis (1989). A 10% uncertainty is assumed for the galactic extinction.

4.1. GRB 980703

The emission of the afterglow of GRB 980703 is dominated by the host galaxy at only few days after the main event. No break has been detected in the optical within this time interval, which means that we can set only a lower limit on the jet opening angle, by requiring t_j to be sufficiently large.

The decay of the optical emission is characterized by a power-law index $\alpha_o = 1.17 \pm 0.25$ (Bloom et al. 1998), or $\alpha_o = 1.39 \pm 0.30$ (Castro-Tirado et al. 1999a), or $\alpha_o = 1.63 \pm 0.12$ (Vreeswijk et al. 1999a), therefore the weighted average index is $\bar{\alpha}_o = 1.53 \pm 0.10$. The slope of the optical spectrum is $\beta_o = 2.71 \pm 0.12$ (Vreeswijk et al. 1999a) at $t = 1.2$ days, and an X -ray decay index $\alpha_x = 1.33 \pm 0.25$ was found by Galama et al. (1998). Thus the observations give $\alpha_x - \bar{\alpha}_o = -0.20 \pm 0.27$. In view of the analytical considerations given in §3.1, the above $\alpha_x - \bar{\alpha}_o$ does not help determining type of external medium and/or location of the cooling break, because it is consistent with:

1. $\alpha_x - \alpha_o \leq -1/4$ (implying $s = 2$ and $\nu_c < \nu_x$),
2. $-1/4 \leq \alpha_x - \alpha_o \leq 0$ (implying $s = 0$, $\nu_c < \nu_x$, $Y > 1$, and $p > 8/3$), and
3. $\alpha_x = \alpha_o$ (implying $\nu_x < \nu_c$, $s = 0, 2$).

It only marginally rules out that $0 \leq \alpha_x - \alpha_o \leq 1/4$, which requires $s = 0$ and $\nu_c < \nu_x$.

For $s = 0$ and $\nu_o < \nu_c$, the observed $\alpha_o = (3p - 3)/4$ requires that $p = 3.15 \pm 0.16$, which implies $\beta_o = (p - 1)/2 = 1.07 \pm 0.08$. Such a spectrum is much harder than observed, therefore consistency between observations and the fireball model can be achieved only if there is a substantial extinction. Given that the galactic extinction toward this afterglow is $E(B - V) = 0.061$ (Bloom et al. 1998), it follows that most this extinction is due to the host galaxy. Vreeswijk et al. (1999a) have shown that the synchrotron power-law spectrum becomes consistent with the observed one for an extinction at source of $A_V = 1.45 \pm 0.13$. At the same time the dereddened optical fluxes lead to $\beta_{ox} = 1.06 \pm 0.04$, which is consistent with the dereddened $\beta_o = (p - 1)/2$, implying that the cooling break is above X -rays. Furthermore Vreeswijk et al. (1999a) have shown that, in the case $\nu_c < \nu_o$, the host extinction required to obtain consistency between the synchrotron shock model and the observed α_o and β_o implies that the dereddened optical emission has $\beta_o < \beta_{ox}$, so that self-consistency within the synchrotron fireball model cannot be reached.

For $s = 2$ and assuming $\nu_o < \nu_c < \nu_x$, we have $\alpha_o = (3p - 1)/4$, therefore the observed α_o requires $p = 2.48 \pm 0.16$ and $\beta_o = (p - 1)/2 = 0.74 \pm 0.08$, which is again much harder than observed. Using the approximations found by Cardelli, Clayton, & Mathis (1989) for the UV interstellar reddening, one can show that dust extinction in the host galaxy ($z = 0.966$) steepens the synchrotron spectrum by $\Delta\beta_o \simeq 1.13A_V$ at the frequency which is red-shifted in the observer V -band. Therefore the synchrotron and observed spectra are consistent if $A_V = 1.74 \pm 0.13$, which is larger than for $s = 0$ models, because pre-ejected wind models yield softer spectra than $s = 0$ models, for the same decay index α . The corresponding dereddened optical emission has $\beta_{ox} = 1.11 \pm 0.04$, which falls between the limiting values allowed by the synchrotron model: $(p - 1)/2$ and $p/2$.

Thus the afterglow of GRB 980703 may be explained by models with homogeneous external media, $\nu_o < \nu_x < \nu_c$, $p \sim 3.1$ and a host extinction in the observer R -band $A_{(1+z)R} = 2.55 \pm 0.23$, or by models with pre-ejected winds, $\nu_o < \nu_c < \nu_x$, $p \sim 2.5$ and host extinction $A_{(1+z)R} = 3.58 \pm 0.24$. We shall leave out the latter case as it is the only one for which we find analytically that an $s = 2$ medium may accommodate the observations.

Figure 1 shows one $s = 0$ model which provides an acceptable fit to the data, except perhaps the radio spectrum, where

the data suggests that the emission is self-absorbed (Vreeswijk et al. 1999a). For a lower limit on the initial jet angle of 0.1 radians, required by the condition that collimation effects are not detectable within the first several days, the implied energy of the ejecta exceeds $\sim 5 \times 10^{51}$ ergs.

4.2. GRB 990123

After the subtraction the host galaxy, the Gunn- r band light-curve of the afterglow of GRB 990123 had a break around $t_b = 2$ days (Kulkarni et al. 1999a). The magnitude of this break, i.e. the difference between the asymptotic logarithmic slopes at late and early times, $\alpha_{o,2} = 1.65 \pm 0.06$ and $\alpha_{o,1} = 1.10 \pm 0.03$, respectively (Kulkarni et al. 1999a), is $\Delta\alpha_o \simeq 0.55 \pm 0.07$. The same break magnitude is implied by the power-law indices found by Castro-Tirado et al. (1999b). The reported slopes of the optical spectrum are $\beta_o = 0.75 \pm 0.23$ at $t = 1.2$ days (Galama et al. 1999), and $\beta_o = 0.8 \pm 0.1$ at $t = 1$ day (Kulkarni et al. 1999a). The optical-to- X -ray spectral slope β_{ox} (defined by $F_\nu \propto \nu^{-\beta_{ox}}$) reported by Galama et al. (1999) is $\beta_{ox} = 0.67 \pm 0.02$ at $t = 1.2$ days, consistent with β_o , therefore at $t \lesssim t_b$ the cooling break must have been outside the optical to X -ray range, or slightly below X -rays. The first BeppoSAX measurement (Heise et al. 1999) and the ASCA data (Murakami et al. 1999) give an X -ray decay index $\alpha_x = 1.17 \pm 0.10$ for $0.2 \text{ d} < t < 2 \text{ d}$, therefore $\alpha_x \simeq \alpha_{o,1}$.

If the break in the optical emission were due to the passage of the ν_c , then $\Delta\alpha_o > 1/4$ implies that $s = 2$, $Y > 1$, an increasing ν_c (see §3.1), and $p = 2.46 \pm 0.08$. Using equation (22) it can be shown that this model yields optical and X -ray decay indices that are consistent with the observations. However it fails in producing the right optical-to- X -ray slope: at $t < t_b$, when $\nu_c < \nu_o$, $\beta_{ox} = p/2 = 1.23 \pm 0.04$, which is inconsistent with the observations. This shows that the passage of ν_c is not a viable explanation for the optical break seen in this afterglow and that this break is due to collimation of ejecta.

More generally, the observed β_{ox} rules out that $\nu_c < \nu_o$, as in this case $\beta_{ox} = p/2$ implies $p = 1.34 \pm 0.02$, which is too small to explain the decay rate of the early ($t < t_j$) optical emission.

If $\nu_o < \nu_c < \nu_x$ then, as discussed in §3.3, the equality of the observed α_o α_x implies that ν_c evolved very slowly in time, which requires an $s = 0$ external medium, $Y > 1$, and $p \sim 8/3$. This value of p is roughly consistent with that required by $\alpha_{o,1} = (3p - 3)/4 = 1.10 \pm 0.03$ (i.e. $p = 2.47 \pm 0.02$).

The last possibility, $\nu_x < \nu_c$, implies that $\beta_{ox} = (p - 1)/2$, thus the observed β_{ox} requires $p = 2.34 \pm 0.04$. Then, if $s = 0$, $\alpha_{o,1} = (3p - 3)/4 = 1.00 \pm 0.03$, while if $s = 2$, $\alpha_{o,1} = (3p - 1)/4 = 1.50 \pm 0.03$. Only the former value is consistent with the observations.

From this analysis one can conclude that a successful model for the afterglow of GRB 990123 is that of a jet interacting with a homogeneous external medium, with parameters such that $\nu_o < \nu_c \lesssim \nu_x$ at $t < t_j$, and $p \sim 2.4$. This index p implies an optical decay index at $t > t_j$ substantially larger than reported by Kulkarni et al. (1999a), but it is quite likely that, due to the short time span of the observations made after $t_j \sim 2$ days, the true $\Delta\alpha_o$ is underestimated.

If the ν_i break were below radio frequencies (ν_r), then the radio-to-optical spectral slope is $\beta_{ro} = (p - 1)/2$; observations give that at $t = 1.2$ days $\beta_{ro} = 0.27 \pm 0.04$, which would require an index $p = 1.54 \pm 0.08$ inconsistent with that required by the optical and X -ray data (see above). Therefore $\nu_r < \nu_i$ for $t < t_j$. As pointed out by Kulkarni et al. (1999a), in this

model the radio emission after $t = 1.2$ days should brighten as a result of the continuous decrease of ν_i , approaching ν_r .

The radio light-curve shown in Figure 2 with dashed line proves that the effects due to collimation of the ejecta are not strong enough to explain the faintness of the radio afterglow observed at $t > 1.2$ days. To this end we assume that there is another radiation mechanism (reverse shock emission – Sari & Piran 1999) that produces the two earliest radio fluxes, and we use these two radio measurements only as upper limits for the forward shock emission. As shown in Figure 2, the K -band fluxes observed after 10 days lie above the model prediction, being inconsistent with an achromatic break resulting from collimated ejecta. This indicates either a shortcoming of the simplest jet model or that the host galaxy emission in the K -band (Kulkarni et al. 1999b) was underestimated.

4.3. GRB 990510

The optical afterglow of GRB 990510 exhibited a break around $t_b = 1.5$ days, whose reported magnitude is $\Delta\alpha_o = 1.80 \pm 0.20$ (Israel et al. 1999) in the V -band, $\Delta\alpha_o = 1.67 \pm 0.02$ (Stanek et al. 1999), to $\Delta\alpha_o = 1.36 \pm 0.05$ (Harrison et al. 1999). The optical asymptotic decay indices found by Harrison et al. (1999) are $\alpha_{o,1} = 0.82 \pm 0.02$ and $\alpha_{o,2} = 2.18 \pm 0.05$. The X -ray decay index was $\alpha_x = 1.42 \pm 0.07$ (Kuulkers et al. 1999) at $0.3 \text{ d} < t < 2 \text{ d}$, while the optical spectral slope was $\beta_o = 0.61 \pm 0.12$ (Stanek et al. 1999) at $t = 0.9$ days. The available data imply an optical-to- X -ray slope $\beta_{ox} = 0.90 \pm 0.04$ at $t = 0.72$ days.

Even the smallest reported $\Delta\alpha_o$ is above $5/4$, therefore the break seen in the optical emission cannot be due to the passage of ν_c (see §3.3). Therefore this break must be caused by collimation of ejecta. The fact that $\beta_o < \beta_{ox}$ implies that ν_c is between optical and X -rays. The same conclusion is suggested by that $\alpha_{o,1} < \alpha_x$, however the X -ray observations were made at times close to t_b , therefore the observed α_x may overestimate the early time, asymptotic α_x .

For $s = 0$, $\alpha_{o,1} = (3p - 3)/4$ requires that $p = 2.09 \pm 0.03$, which is consistent with observed $\alpha_{o,2}$. This p implies an optical spectral slope $\beta_o = (p - 1)/2 = 0.55 \pm 0.02$, consistent with the observations. The observed β_{ox} is close to $p/2$, therefore the cooling break is closer to optical than to X -ray frequencies. For $s = 2$, $\alpha_{o,1} = (3p - 1)/4$ requires that $p = 1.43 \pm 0.03$, implying that $\beta_o = (p - 1)/2 = 0.22 \pm 0.02$, which is inconsistent even with the softest optical spectrum reported by Stanek et al. (1999) $\beta_o = 0.46 \pm 0.08$. It also implies $\beta_{ox} \leq p/2 = 0.72 \pm 0.02$, also inconsistent with the observations. Thus a pre-ejected wind medium is ruled out.

Therefore the afterglow of GRB 990510 can be accommodated by a model with $s = 0$, $\nu_o \lesssim \nu_c < \nu_x$ and $p \sim 2.1$. The very flat radio-to-optical spectrum at $t = 0.72$ days (Figure 3) requires that $\nu_r < \nu_i < \nu_o$. Note that the model shown in Figure 3 fits well the X -ray data, the light-curve steepening being very slow.

4.4. GRB 991216

The optical decay index of the afterglow of GRB 991216 was $\alpha_{o,1} = 1.22 \pm 0.04$ (Halpern et al. 2000, Sagar et al. 2000) at $t < t_b = 2$ days. Halpern et al. have shown that a broken power-law optical light-curve with $\alpha_{o,2} = 1.53 \pm 0.05$ at $t > t_b$ plus the contribution $R = 24.8 \pm 0.1$ from a galaxy located at ~ 1 arcsecond from the optical transient explains well the available observations. Sagar et al. (2000) find that two measurements made after t_b are dimmer by 2σ than the power-law

extrapolation from earlier fluxes. Therefore there is evidence that the afterglow of GRB 991216 had a steepening of the optical emission decay, although an un-broken power-law optical emission has not been shown clearly to be inconsistent with the observations.

The X -ray data span 1.3 decades in time before t_b , and have $\alpha_x = 1.62 \pm 0.07$ (Frail et al. 2000, Halpern et al. 2000), leading to $\alpha_x - \alpha_{o,1} = 0.40 \pm 0.08$. The optical spectrum is puzzling, exhibiting a turn-over at the J -band at $t \simeq 1.5$ days (Frail et al. 2000, Halpern et al. 2000), although the J and K -band measurements reported by Garnavich et al. (2000) restore a power-law optical spectrum, with slope $\beta_o = 0.58 \pm 0.08$ at $t = 1.7$ days. According to Garnavich et al. (2000), systematic errors in the galactic extinction could lead to $\beta_o = 0.87 \pm 0.08$. The optical-to- X -ray spectral slope is $\beta_{ox} = 0.80 \pm 0.10$ (Garnavich et al. 2000, Halpern et al. 2000).

The faster decay seen at X -ray than at optical frequencies before t_b implies that $\nu_o < \nu_c < \nu_x$ and, as discussed in §3.3, ν_c must decrease in time, $Y < 1$, and the external medium must be homogeneous. That ν_c is between optical and X -ray frequencies is also suggested by $\beta_{ox} - \beta_o = 0.22 \pm 0.13$, as noted by Halpern et al. (2000).

If the optical light-curve break were due to the passage of ν_c , then $\Delta\alpha_o = 1/4$ for $Y < 1$ (see §3.1), which is consistent with the observed $\Delta\alpha_o = 0.31 \pm 0.06$. However, at $t \sim t_b$, when $\nu_c \sim \nu_o$, the optical-to- X -ray slope should be $\beta_{ox} = p/2 = 1.32 \pm 0.03$, inconsistent with the observations. Therefore the break in the optical emission of this afterglow is not due to the passage of ν_c , but to collimation of the ejecta.

For $\nu_o < \nu_c$ at $t < t_b$, the analytical optical decay index is $\alpha_{o,1} = (3p - 3)/4$. Then the observed $\alpha_{o,1}$ requires that $p = 2.63 \pm 0.05$, which implies that $\beta_o = (p - 1)/2 = 0.82 \pm 0.03$. Such a spectrum is *softer* by 3σ than observed, a discrepancy which cannot be due to extinction in the host galaxy. The above value of p implies that, at $t > t_j$, $\alpha_{o,2} = 2.63 \pm 0.05$, which is larger than observed by 2σ . Furthermore, for $s = 0$, $\nu_o < \nu_c < \nu_x$, and at $t < t_j$, one expects (see §3.3) that $\alpha_x - \alpha_{o,1} \leq 1/4$, which is 2σ below the observed value. All these marginal consistencies between the fireball model and the temporal/spectral features of the afterglow of GRB 991216 suggest that it may be difficult to find models with an acceptable χ^2 .

The observed decay index of the radio emission $\beta_r = 0.82 \pm 0.02$ (Frail et al. 2000) at $t \gtrsim 1$ day would require that, at these times, $\nu_i < \nu_r$. This implies that the radio-to-optical spectral slope at $t \sim 2$ days is $\beta_{ro} = \beta_o = 0.58 \pm 0.08$, while the observations give $\beta_{ro} = 0.20 \pm 0.05$. The discrepancy is large enough to suggest that the fireball model cannot accommodate the optical and all the radio data. It is possible that, as in the case of GRB 990123, the early radio emission is dominated by the reverse shock. Furthermore, the last radio measurements are at $t > 40$ days, past the last available optical detection. It is entirely possible that, at such large times, there are significant departures from the standard model of uniform ejecta interacting with an isotropic medium.

For these reasons we search for models that accommodate the radio data excluding either the first four measurements or the last three ones. Figure 4 shows a model for the former case, with a marginally acceptable $\chi^2 = 56$ for 40 degrees of freedom. As in the case of GRB 990123, the R -band model emission after 10 days falls below the observed fluxes, implying either a departure from the standard jet model, or an underestimation of the contaminating flux from a close galaxy (Halpern et

al. 2000). Note that the flat radio emission seen between 10 and 40 days provides further evidence for a jet undergoing lateral spreading, otherwise the radio emission should have evolved as $F\nu \propto \nu^{1/2}$.

Figure 5 shows an alternate model to the afterglow of GRB 991216, obtained in the latter case, i.e. when the last three radio measurements are left out. In this model the initial jet opening is so small that the emission steepening due to collimation effects occurs before the earliest measurements. The rather unacceptable $\chi^2 = 64$ for 41 degrees of freedom of this model is due to that it requires the decay indices α_ν at $\nu > \nu_i$ to be equal, a feature which is inconsistent with the early optical observations ($\alpha_x - \alpha_{o,1} = 0.40 \pm 0.08$), but allowed by the late ones ($\alpha_x - \alpha_{o,2} = 0.09 \pm 0.09$). Also note that this model cannot explain the $t_b \sim 2$ days optical light-curve steepening suggested by Sagar et al. (2000) and Halpern et al. (2000).

4.5. Parameter Ranges and Afterglow Energetics

The parameters of the models that yield acceptable fits to the afterglows of GRB 980703, 990123, and 990510, defined by a probability $erf(\sqrt{2})$ (i.e. the 2σ tail of the Gaussian distribution) of yielding a larger χ^2 than observed, and the best (though only marginally acceptable) fits for GRB 991216 are summarized in Figures 6, 7, and 8. Figure 7 shows that, when the effects arising from collimation of ejecta have been seen in the optical emission, the initial jet opening angle ranges from less than 1 deg to 3 deg. In all cases, the external medium density was found to be below 1 cm^{-3} , indicating that these GRBs did not occur in dense molecular clouds but. Figure 8 shows that ε_e , the parameter for the electron fractional energy, ranges from less than 1% to more than 10%, while ε_B , the parameter of the magnetic field intensity, is poorly constrained, ranging between 10^{-6} and 0.1.

Figure 9 shows the jet energy corresponding to the parameters E_0 and θ_0 versus the γ -ray efficiency of the afterglow, defined as the ratio of the energy E_γ seen in γ -rays to the total fireball energy $E_\gamma + E_0$, assuming that the jet is uniform (i.e. there are no angular gradients). The E_γ was calculated from the reported fluences Φ_γ above 20 keV (Kippen et al. 1998, 1999) and the measured redshifts (see captions of Figures 1–4):

1. GRB 980703 – $\Phi_\gamma = 4.6 \times 10^{-5} \text{ erg cm}^{-2}$ and $z = 0.966$ lead to $E_\gamma = 1.1 \times 10^{53} \text{ ergs}$.
2. GRB 990123 – $\Phi_\gamma = 5.1 \times 10^{-4} \text{ erg cm}^{-2}$ and $z = 1.60$ imply $E_\gamma = 3.4 \times 10^{54} \text{ ergs}$.
3. GRB 990510 – $\Phi_\gamma = 2.6 \times 10^{-5} \text{ erg cm}^{-2}$ and $z = 1.62$ yield $E_\gamma = 1.7 \times 10^{53} \text{ ergs}$.
4. GRB 991216 – $\Phi_\gamma = 2.6 \times 10^{-4} \text{ erg cm}^{-2}$ and $z = 1.02$ imply $E_\gamma = 6.7 \times 10^{53} \text{ ergs}$.

Note from Figure 9 that the jet energies range from 10^{49} to 10^{52} ergs, and that the minimum efficiency for GRB 990510 and GRB 991216 are 2–4%, while for GRB 990123 it is slightly less than 10%.

With the exception of the afterglow of GRB 990510, the radiative losses for the models shown in Figures 6–8 are negligible, below few percent. For GRB 990510 these losses amount to about 30%. Inverse Compton scattering is the main electron radiative cooling mechanism, determining the evolution of the cooling break frequency ν_c , for the afterglow of GRB 990510, at all times shown in Figure 3, and for that of GRB 990123 until several days. Radiative cooling is mainly due to synchrotron emission in the afterglows of GRB 970803 and 991216.

5. CONCLUSIONS

We have developed a numerical model for the calculation of dynamics and synchrotron emission of collimated, lateral spreading GRB remnants interacting with an external medium. The remnant is assumed uniform (i.e. the angular gradients of density and energy are zero). We have also assumed that, at any time, the electron distribution in the ejecta is well described by a broken power-law. This model was used to determine the isotropic equivalent energy E_0 , initial jet opening angle θ_0 , external medium density n , exponent $-p$ of the power-law distribution of injected electrons, and parameters ε_e and ε_B quantizing the fractional energy in electrons and in magnetic field, respectively, for the afterglows of GRB 980703, 990123, 990510, and 991216.

As illustrated in Figures 6 and 7, the parameters θ_0 and p are well constrained by the observations, because the effects of collimation are seen at a time which depends strongly on θ_0 (eq. [27]), while p determines the afterglow decay rate, which is well constrained by observations. Other model parameters – E_0 , n , and ε_B – are less well constrained, their allowed values spanning at least a decade (see Figures 7 and 8). This is due to that observations made in three frequency domains (radio, optical, and X -ray) provide at most three constraints for four unknowns (E_0 , n , ε_e , and ε_B).

For three of the above mentioned afterglows, the external medium densities resulting from numerical fits are around 10^{-3} cm^{-3} (Figure 7). For those with optical light-curve breaks, we find an initial jet opening angle below 3 deg (Figure 7), and jet energies in the range $10^{50.7}$ to $10^{51.5}$ ergs, if their γ -ray efficiencies are smaller than 10% (Figure 9). From the analysis of the radio data covering 450 days, Frail, Waxman & Kulkarni (2000) found for the afterglow of GRB 970508 a jet energy of 5×10^{50} ergs, which is the lower limit given above, a jet initial half-angle of ~ 30 deg, and an external medium density around 1 cm^{-3} .

The minimum γ -ray efficiency for the collimated afterglows analyzed here ranges from less than 1% to about 8% (Figure 9). The former limit is within the reach of current calculations of internal shock efficiency (Kumar 1999, Lazzati et al. 1999, Panaiteescu, Spada & Mészáros 1999), but the latter exceeds it. However, if the energy is not distributed isotropically within the jet opening, such that we are biased toward detecting more often those bursts arising from ejecta whose energy-per-solid angle peaks toward the observer, then the minimum required efficiency may be significantly smaller.

We note that if the optical flash of GRB 990123 was due to a reverse shock propagating in the ejecta (Sari & Piran 1999), and if the peak of this flash, seen at $t \sim 50$ seconds, corresponds to the fireball deceleration timescale, then the isotropic energy and external density shown in Figure 7 imply that the fireball initial Lorentz factor was $\Gamma_0 \gtrsim 1000$. Alternatively, the optical flash may have been caused by internal shocks in an unstable wind (Mészáros & Rees 1999), in which case Γ_0 is uncertain.

A.P. acknowledges support from the Lyman Spitzer Jr. fellowship. The work of P.K. is supported in part by NSF grant phy-0070928. The authors commend the work of Jochen Greiner, who maintains a very useful compilation of the available information on GRB afterglows at <http://www.aip.de:8080/~jcg/grbgen.html>.

REFERENCES

Beloborodov, A. 2000, *ApJ*, 539, L25

Beuermann, K. et al. 1999, *A&A*, 352, L26

Bloom, J. et al. 1998, *ApJ*, 508, L21

Bloom, J. et al. 2000, GCN #756

Campins, H., Rieke, G., & Lebofsky, M. 1985, *AJ*, 90, no 5, 896

Cardelli, J., Clayton, G., & Mathis, A. 1989, *ApJ*, 345, 245

Castro-Tirado, A. et al. 1999a, *ApJ*, 511, L85

Castro-Tirado, A. et al. 1999b, *Science*, 283, 2069

Corbet, R. et al. 1999, GCN #506

Djorgovski, S. et al. 1998, *ApJ*, 508, L17

Djorgovski, S. et al. 1999, GCN #510

Frail, D. et al. 1999, GCN #141

Frail, D., Waxman, E., & Kulkarni, S. 2000, *ApJ*, 537, 191

Frail, D. et al. 2000, *ApJ*, 538, L129

Fruchter, A. et al. 1999, GCN #386

Fruchter, A. et al. 2000, GCN #757

Fukugita, M., Shimasaku, K., & Ichikawa, T. 1995, *PASP*, 107, 945

Galama, T. et al. 1998, GCN #145

Galama, T. et al. 1999, *Nature*, 398, 394

Garnavich, P. et al. 2000, *ApJ*, in press (astro-ph/0003429)

Halpern, J. et al. 2000, *ApJ*, in press (astro-ph/0006206)

Harrison, F. et al. 1999, *ApJ*, 523, L121

Heise, J. et al. 1999, IAUC 7099, GCN #202

Israel, G. et al. 1999, *A&A*, 348, L51

Kelson, D. et al. 1999, IAUC 7096

Kippen, R. et al. 1998, GCN #143

Kippen, R. et al. 1999, GCN #224, #322, #504

Kulkarni, S. et al. 1999a, *Nature*, 398, 389

Kulkarni, S. et al. 1999b, *ApJ*, 522, L97

Kumar, P. 1999, *ApJ*, 523, L113

Kumar, P. & Panaiteescu, A. 2000, *ApJL*, 541, L9

Kuulkers, E. et al. 2000, *ApJ*, 538, 638

Lazzati, D., Ghisellini, G., & Celotti, A., 1999, *MNRAS* 309, L13

Mathis, J. 1990, *ARA&A*, 28, 37

Mészáros , P. & Rees, M.J. 1994, *ApJ*, 430, L93

Mészáros , P. & Rees, M.J. 1999, *MNRAS*, 306, L39

Murakami, T. et al. 1999, GCN #228

Odewahn, S. et al. 1999, GCN #261

Panaiteescu, A., Mészáros , P., & Rees, M.J. 1998, *ApJ*, 503, 314

Panaiteescu, A., Spada, M., & Mészáros , P. 1999, *ApJ* 522, L105

Panaiteescu, A. & Kumar, P. 2000, *ApJ*, 543, in press

Pietrzynski, G. & Udalski, A. 1999, GCN #319, #328

Piro, L. 1999, GCN #500

Rhoads, J. 1999, *ApJ*, 525, 737

Rol, E. et al. 1999, GCN #491

Sagar, R., Mohan, V., Pandey, A., & Castro-Tirado, A. 2000, *BASI*, 28, 15

Sari, R., Piran, T., & Narayan, R. 1998, *ApJ*, 497, L17

Sari, R. & Piran, T. 1999, *ApJ*, 517, L112

Sari, R., Piran, T., & Halpern, J. 1999, *ApJ*, 519, L17

Schaefer, B. 2000, GCN #517

Schild, R. 1977, *AJ*, 82, 337

Stanek, K., Garnavich, P., Kaluzny, J., Pych, W., & Thompson, I. 1999, *ApJ*, 522, L39

Takeshima, T. 1999, GCN #478

Vreeswijk, P. et al. 1999a, *ApJ*, 523, 171

Vreeswijk, P. et al. 1999b, GCN #310

Vreeswijk, P. et al. 2000, GCN #751

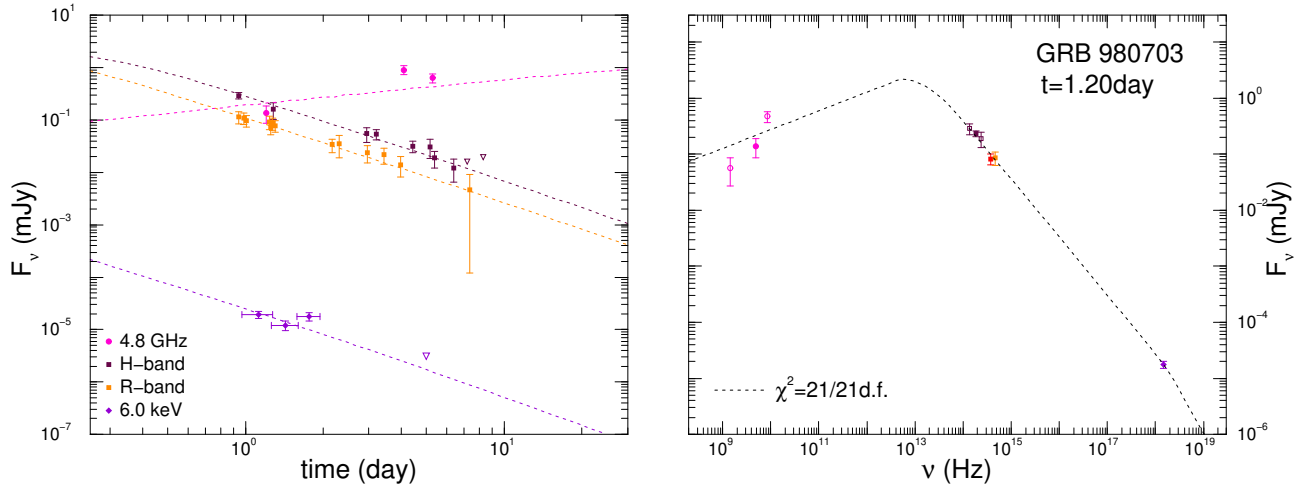


FIG. 1.— Light-curves and $t = 1.20$ day spectrum for the afterglow of GRB 980703 ($z = 0.966$). The radio data were taken from Frail et al. (1999). We assumed 20-40% uncertainty when no errors were reported, the larger errors being for earlier or lower frequency observations, the smaller for later or higher frequencies. The optical fluxes were calculated from the data published by Bloom et al. (1998), Castro-Tirado et al. (1999a), and Vreeswijk et al. (1999a). The host galaxy contribution $R = 22.58 \pm 0.06$, $I = 21.95 \pm 0.20$, $J = 20.87 \pm 0.10$, $H = 20.27 \pm 0.17$ and $K = 18.36 \pm 0.13$ (Vreeswijk et al. 1999a) is subtracted. The optical fluxes were corrected for galactic extinction with $E(B - V) = 0.061$ (Bloom et al. 1998), and for the host galaxy extinction inferred by Vreeswijk et al. (1999a): $A_V = 1.45 \pm 0.13$. The X-ray fluxes were taken from Vreeswijk et al. (1999a). Triangles indicate 2σ upper limits. For the afterglow spectrum (right panel), measurements closest to $t = 1.20$ days were extrapolated to this time, using $F_\nu \propto t^{1/2}$ at radio frequencies, and the temporal indices α reported in the above references. The model shown has $\chi^2 = 21$ for 21 df and the following parameters: $E_0 = 1.9 \times 10^{54}$ erg, $n = 8.0 \times 10^{-4}$ cm $^{-3}$, $\varepsilon_e = 7.0 \times 10^{-2}$, $\varepsilon_B = 9.5 \times 10^{-4}$, $p = 3.08$. The initial jet angle is lower bounded by the condition that no effects of collimation are seen until the later available data, which leads to $\theta_0 \gtrsim 0.1$ rad. Radiative losses until 10 days amount to 0.4%. Synchrotron emission is the main electron radiative cooling mechanism at all times shown here.

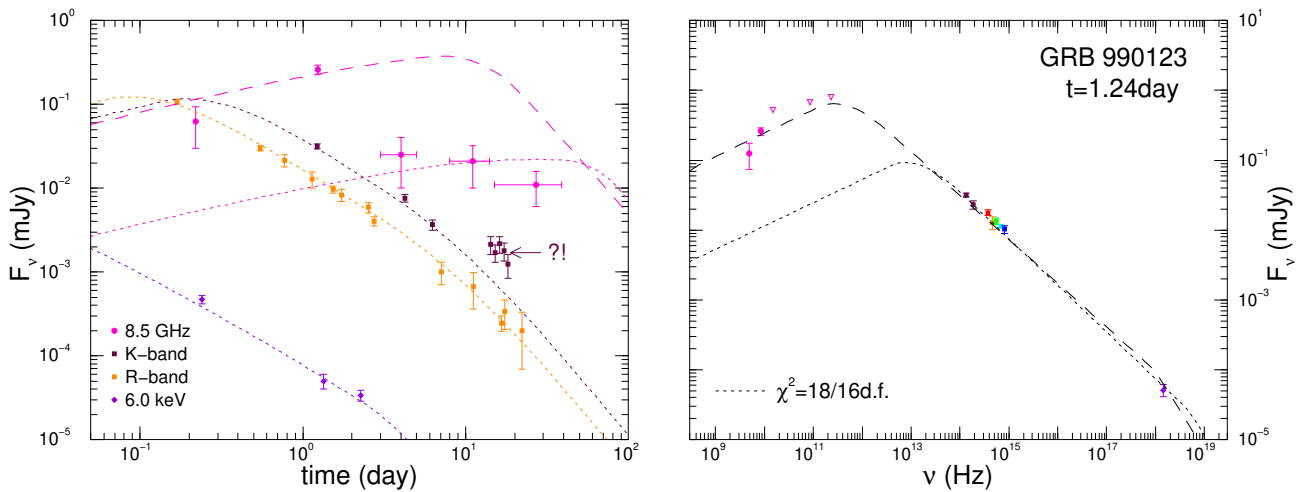


FIG. 2.— Light-curves (left panel) and $t = 1.24$ day spectrum (right panel) for the afterglow of GRB 990123 ($z = 1.61$). The radio data were taken Kulkarni et al. (1999b). The optical fluxes were calculated from the magnitudes reported by Kulkarni et al. (1999a), by subtracting a host galaxy contribution of $F_r = 0.5 \pm 0.1$ μ Jy and $K = 22.1 \pm 0.3$, and the HST measurement reported by Odewahn et al. (1999). Optical fluxes were corrected for a galactic extinction of $A_r = 0.04$ (Kulkarni et al. 1999a). The X-ray fluxes were calculated from the 2-10 keV fluxes reported by Heise et al. (1999) and Murakami et al. (1999), using the quoted spectral indices and assuming a 10% error. Other data, used for the spectrum shown in the right panel, were taken from Galama et al. (1999) and Castro-Tirado et al. (1999b), and were extrapolated to $t = 1.24$ days using the optical decay indices given in Castro-Tirado et al. (1999b). For radio data the extrapolation was done using the analytically expected behavior $F_\nu \propto t^{1/2}$. Triangles indicate 2σ upper limits. The model shown has $\chi^2 = 18$ for 16 df, excluding the first two radio measurements and the group of late K -band observations, and parameters: $E_0 = 8.9 \times 10^{53}$ erg, $\theta_0 = 4.3 \times 10^{-2}$ rad, $n = 8.1 \times 10^{-4}$ cm $^{-3}$, $\varepsilon_e = 0.14$, $\varepsilon_B = 1.7 \times 10^{-4}$, $p = 2.34$. 1.0% of the remnant energy is radiated until 30 days. Inverse Compton scatterings dominate the electron radiative cooling until $t \simeq 6.5$ days. The model shown with it dashed line yields a good fit to the optical and X-ray data, but matches only the first two radio measurements, over-predicting the radio emission after 1 day.

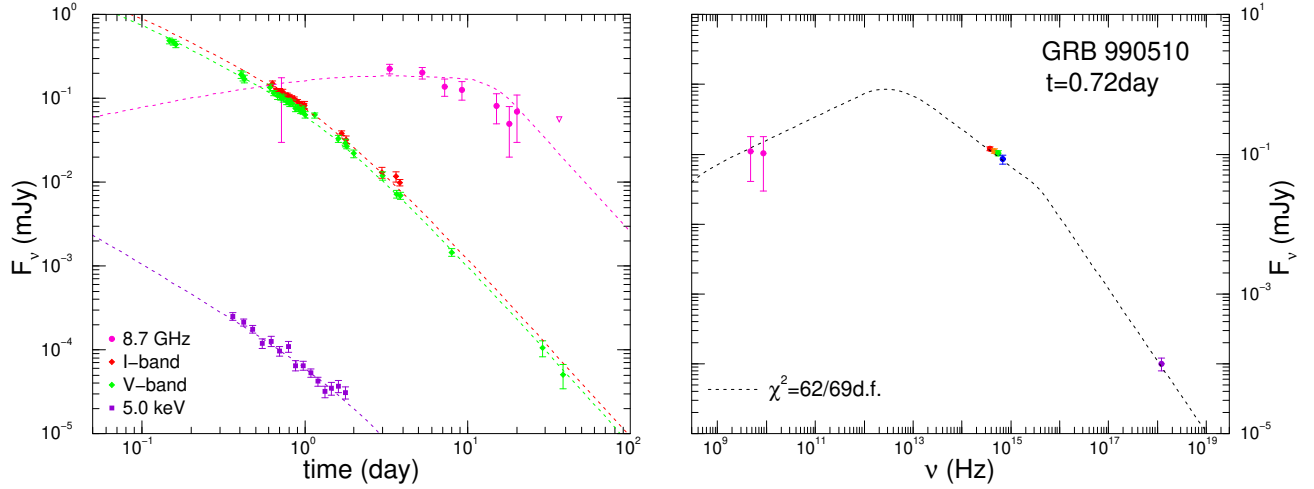


FIG. 3.— Light-curves and $t = 0.72$ day spectrum for the afterglow of GRB 990510 ($z = 1.62$). The radio data were taken from Harrison et al. (1999). The triangle indicates a 2σ upper limit. The optical fluxes were obtained from the magnitudes reported by Beuermann et al. (1999), Fruchter et al. (1999), Harrison et al. (1999), Israel et al. (1999), Pietrzynski & Udalski (1999), and Stanek et al. (1999). These fluxes were corrected for dust extinction with $E(B - V) = 0.20$ (Harrison et al. 1999, Stanek et al. 1999). The uncertain, small contribution of the host galaxy of $V_{gta}28.0$ (Bloom et al. 2000, Fruchter et al. 2000) was ignored. The X-ray fluxes were taken from Kuulkers et al. (2000). The model shown has $\chi^2 = 62$ for 69 df, and parameters: $E_0 = 1.9 \times 10^{54}$ erg, $\theta_0 = 3.9 \times 10^{-2}$ rad, $n = 0.22 \text{ cm}^{-3}$, $\varepsilon_e = 7.2 \times 10^{-2}$, $\varepsilon_B = 3.3 \times 10^{-5}$, $p = 2.05$. The radiative losses until 40 days amount to 28%. At all times shown here, inverse Compton scatterings is the dominant electron radiative cooling mechanism.

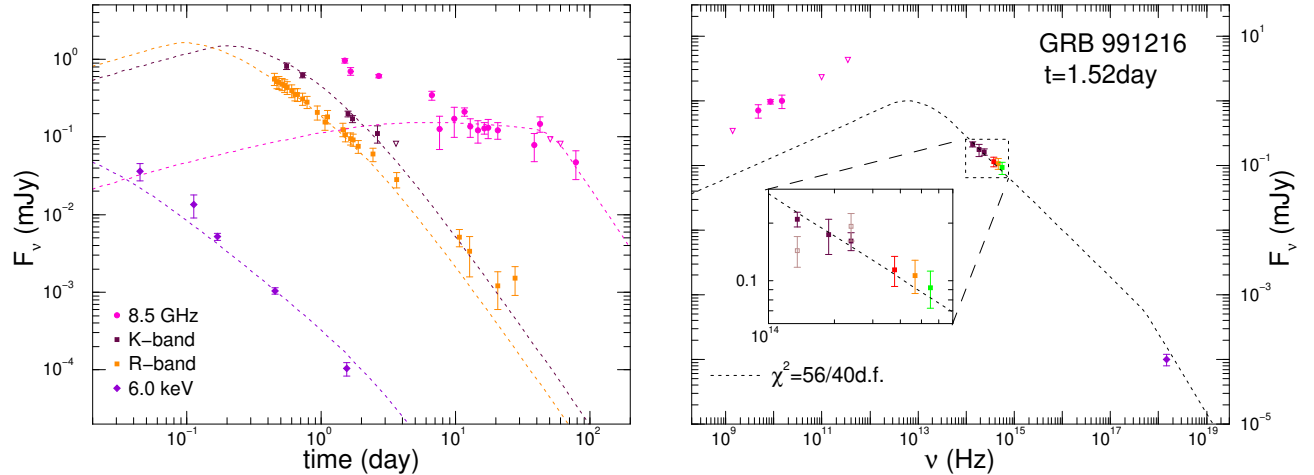


FIG. 4.— Light-curves and $t = 1.52$ day spectrum for the afterglow of GRB 991216 ($z = 1.02$) and for a model obtained by leaving out the first four radio measurements. The radio data were taken from Rol et al. (1999) and Frail et al. (2000). The optical fluxes were calculated from the data published by Garnavich et al. (2000), Halpern et al. (2000), Sagar et al. (2000), and Schaefer (2000). We subtracted the contamination from a galaxy located near the OT, estimated by Halpern et al. (2000) at $R = 24.8 \pm 0.1$. The host galaxy, identified by Vreeswijk et al. (2000), has $R = 26.9 \pm 0.4$. Optical fluxes were corrected for a galactic extinction of $E(B - V) = 0.63$ (Garnavich et al. 2000, Halpern et al. 2000). The X-ray fluxes were calculated from the 2–10 keV fluxes reported by Corbet et al. (1999), Piro et al. (1999), and Takeshima et al. (1999) (the very small errors they report were increased to 10%), using an X-ray spectral slope $\beta = 1.1$ (Takeshima et al. 1999). For the afterglow spectrum, the available measurements closest to $t = 1.52$ days were extrapolated to this time using the temporal power-law scalings quoted in the above references. The J and K measurements of Halpern et al. (2000) are shown with open symbols, while the measurements made by Garnavich et al. (2000), which imply a power-law spectrum, are indicated with filled symbols. For the low frequency domain, triangles indicate 3σ (2σ) upper limits in the left (right) panel. The model shown has $\chi^2 = 56$ for 40 df. It does not accommodate well the last four R -band data, which yield $\Delta\chi^2 = 14$ (without them $\chi^2 = 42$ for 36 df). The parameters of this model are: $E_0 = 1.6 \times 10^{54}$ erg, $\theta_0 = 2.2 \times 10^{-2}$ rad, $n = 2.4 \times 10^{-4} \text{ cm}^{-3}$, $\varepsilon_e = 5.6 \times 10^{-2}$, $\varepsilon_B = 7.0 \times 10^{-3}$, $p = 2.46$. The remnant radiates 1.3% of its energy until 80 days. The radiative electron cooling is due mainly to synchrotron losses at all times shown here.

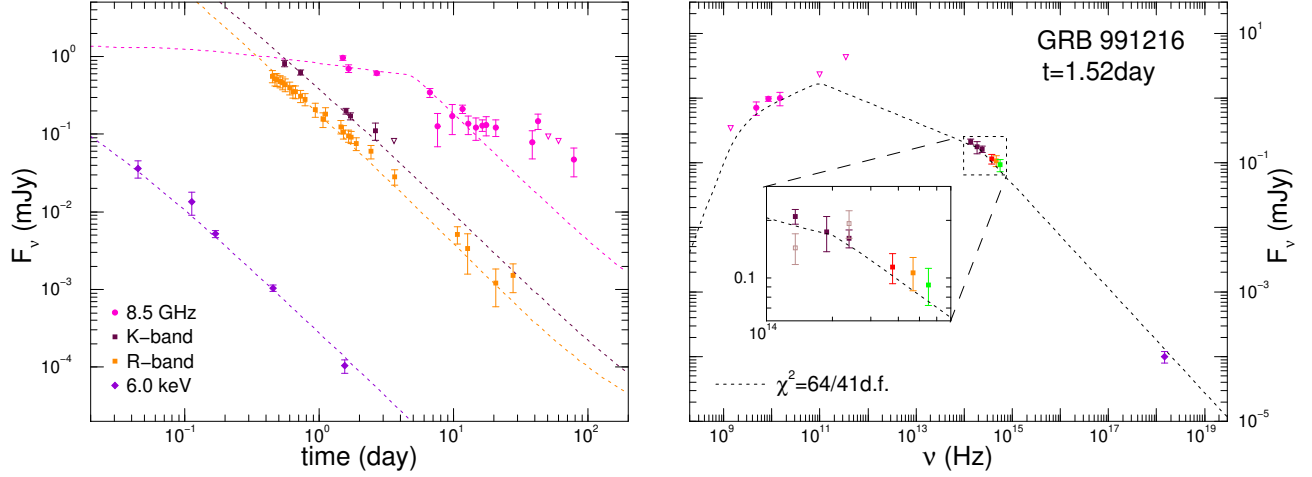


FIG. 5.— Light-curves and spectrum for the afterglow of GRB 991216 and a model obtained by leaving out the last three radio measurements. See Figure 3 for details about the data. In this model a very narrow jet undergoes significant lateral spreading even at the earliest times, therefore the light-curve decay indices α are the same at all frequencies above the injection break ν_i , which falls below $\nu = 8.5$ GHz at several days. The cooling break frequency ν_c is in the NIR-optical range at all times shown here. This model has $\chi^2 = 64$ for 41 df, thus being only marginally acceptable, and parameters: $E_0 = 2.1 \times 10^{54}$ erg, $\theta_0 = 5.9 \times 10^{-3}$ rad, $n = 3.4 \times 10^{-2}$ cm $^{-3}$, $\epsilon_e = 8.8 \times 10^{-3}$, $\epsilon_B = 0.11$, $p = 1.61$. Radiative losses until 80 days amount to 2.8%. As for Figure 4, at all times shown here, synchrotron emission is the dominant electron radiative cooling mechanism.

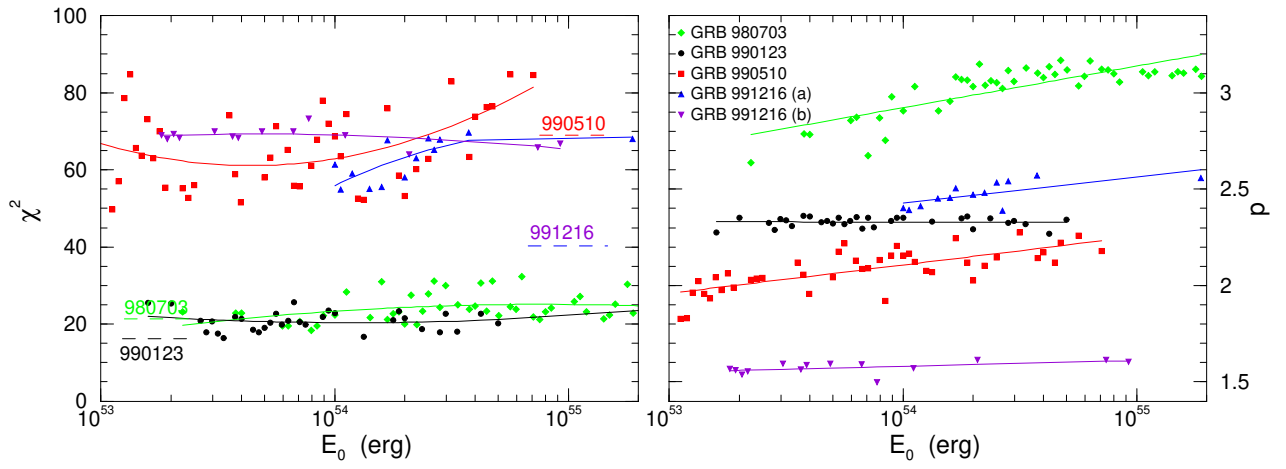


FIG. 6.— Left panel: χ^2 for various isotropic energies E_0 of the ejecta, with all other parameters left free to yield the best fit. Horizontal lines show the degrees of freedom for each afterglow. For the models shown here, the probability of obtaining a larger χ^2 is at least 5%, with the exception of GRB 991216, where an upper cut-off of $\chi^2_{max} = 73$ for 40 df was used. The sets of parameters for this afterglow, obtained by excluding the first four radio measurements (see Figure 4) are labeled GRB 991216(a), while those obtained by excluding the last three radio data (Figure 5) are labeled GRB 991216(b). Also shown are the general trends of χ^2 with E_0 , obtained through a quadratic fit in log-linear coordinates. The χ^2 increases rapidly for energies outside the ranges shown here. Right-panel: the electron index p for the same models. This index is constrained by the optical and X-ray temporal decay indices, and is thus largely independent of other model parameters. The curves indicate log-linear fits.

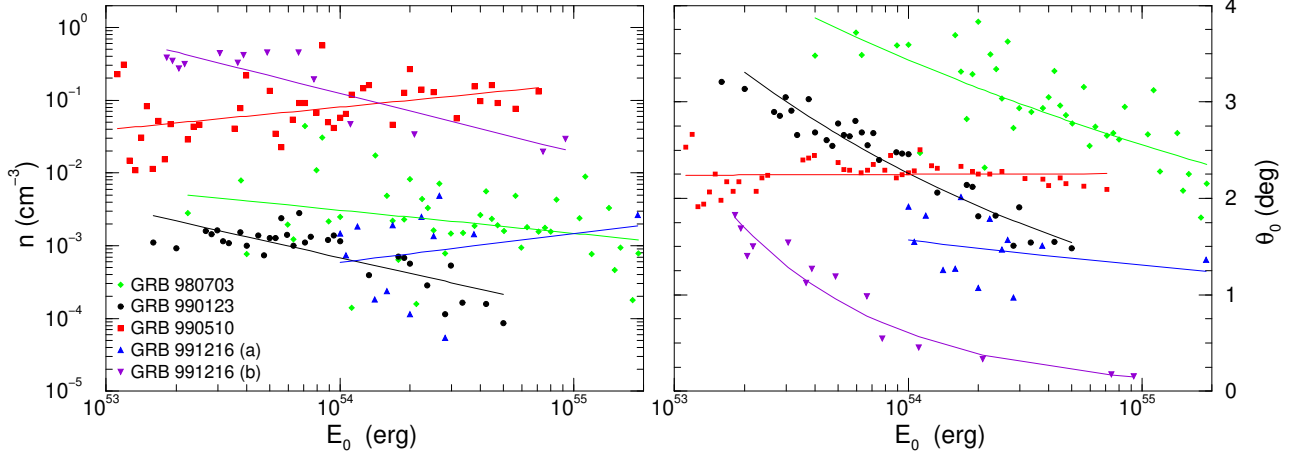


FIG. 7.— Dynamic parameters θ_0 (jet initial opening) and n (external medium density) for the models shown in Figure 5, for various isotropic energies of ejecta E_0 . The decay of the afterglow of GRB 980703 did not show evidence for collimation of ejecta until several days. The jet opening angles θ_0 shown for this case were obtained by requiring that $t_j = 5$ days (see eq. [27]), therefore they are lower limits of the true θ_0 . Note that, for all these afterglow models, $n < 1 \text{ cm}^{-3}$. The curves are linear fits in log-log coordinates and show the general trends with E_0 .

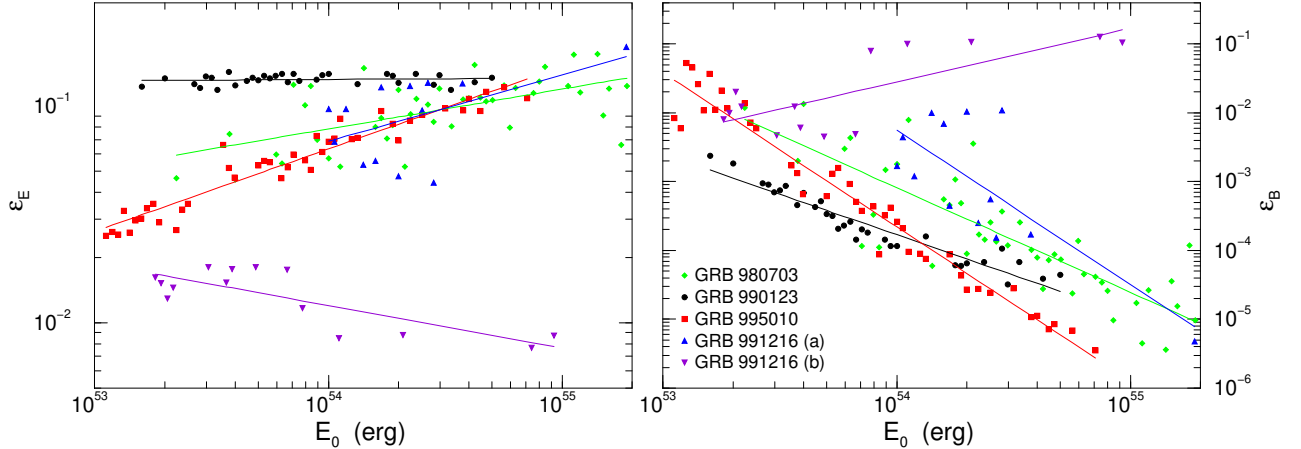


FIG. 8.— Energy release parameters ε_e (which gives the fractional energy in electrons) and ε_B (fractional energy in magnetic field) for the models in Figures 5 and 6. Linear fits in log-log coordinates are also shown to illustrate the trend in each parameter.

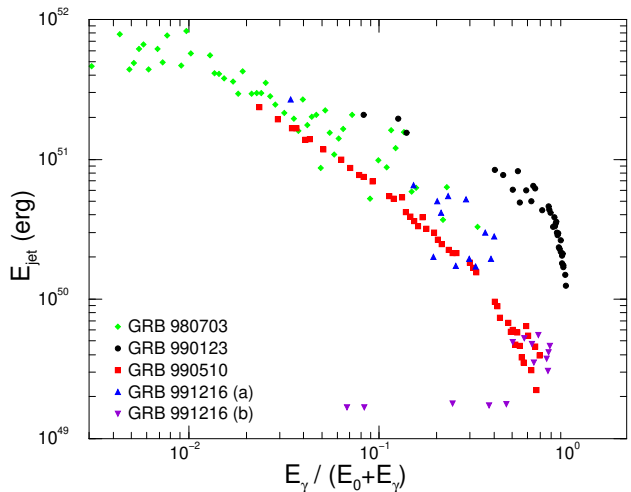


FIG. 9.— Jet energy $E_{jet} \simeq (\theta_0/2)^2 E_0$ and the GRB radiative efficiency for the models whose parameters are shown in Figures 6, 7, and 8. The radiative efficiency is the ratio of the energy E_γ released in γ -rays during the main event and the initial fireball energy $E_\gamma + E_0$, where E_0 results from fits to the afterglow emission. For GRB 980703 we used jet angles θ_0 which yield $t_j = 5$ days, as shown in Figure 7.